83

N91-19196

Burst Annealing of High Temperature GaAs Solar Cells

P.R. Brothers and W.E. Horne
Boeing
Seattle, WA

Introduction

One of the major limitations of solar cells in space power systems is their vulnerability to radiation damage. One solution to this problem is to periodically heat the cells to anneal the radiation damage. Annealing has been demonstrated with silicon cells [ref. 1]. The obstacle to annealing of GaAs cells has been their susceptibility to thermal damage at the temperatures required to completely anneal the radiation damage. GaAs cells with high temperature contacts and encapsulation have been developed under a joint effort by Boeing and the Kopin Corp [ref. 2]. The cells tested are designed for concentrator use at 30 suns AM0. The circular active area is 2.5 mm in diameter for an area of 0.05 cm^2. Typical one sun AM0 efficiency of these cells is over 18%. They have been demonstrated to be resistant to damage after thermal excursions in excess of 600°C. This high temperature tolerance should allow these cells to survive the annealing of radiation damage. A limited set of experiments were devised to investigate the feasibility of annealing these high temperature cells. The effect of repeated cycles of electron and proton irradiation was tested. The damage mechanisms were analyzed. Limitations in annealing recovery suggested improvements in cell design for more complete recovery. These preliminary experiments also indicate the need for further study to isolate damage mechanisms.

The primary objective of the experiments was to demonstrate and quantify the annealing behavior of high temperature GaAs cells. Secondary objectives were to measure the radiation degradation and to determine the effect of repeated irradiation and anneal cycles.

Test Conditions

The test plan illustrated in figure 1 was developed to guide the use of a limited number of cells available for testing in a limited period of time. The GaAs cells were divided into three groups of four cells each. There was a control group, a thermal control group, and an irradiation test group. The control group was used to verify the performance of the measurement equipment and to factor out slight changes in the behavior of the solar simulator. A Spectrolab XT10 solar simulator was used in conjunction with a custom built load bank to make IV curve measurements. The irradiation test group was exposed to electrons, annealed, exposed to protons, and annealed a second time. The thermal control group was annealed at the same time

as the irradiation group but not exposed to irradiation. In this way any degradation from thermal exposure could be evaluated as a factor separate from the radiation effects.

The Boeing Physical Sciences Research Center linear accelerator was used as a source of electrons for the electron irradiation. The cells were exposed to 1×10^{15} 10 Mev e^-/cm^2. After steps to measure and anneal the cells, they were then exposed to 2×10^{11} 1.7 Mev p^+/cm^2 using a Van De Graff accelerator at the University of Washington as a source. Electron dose was measured using thermal luminescence dosimetry. At the University of Washington, a solid state detector was used in conjunction with a Faraday cup to measure proton dose. For each type of radiation the exposure was in two steps with an intermediate step to check cell degradation by measuring short circuit current in ambient room lighting. The target degradation for demonstrating thermal annealing was a 20% loss in maximum power.

The annealing test fixture is shown in figure 2. The fixture was mounted in a high vacuum chamber which was evacuated to less than 5×10^{-5} torr during the annealing cycles. Heating was accomplished by passing a current through a graphite bar. The bar had a slot machined in it to accommodate the solar cells. Since the cells were recessed completely in the slot, they were tightly coupled thermally to the heater bar. The temperature was monitored by two thermocouples. Only the center third of the heater bar was used in order to maintain a uniform temperature. A typical annealing thermal profile curve is shown in figure 3. The temperature rises from room ambient to the target temperature within 10 to 15 seconds. The cool down was relatively slower due to limited radiative cooling, but still dropped below 100°C within two minutes.

Results

Light IV curves were measured for the 12 GaAs cells before the first irradiation. After the electron and again after the proton irradiations, the four control cells and the four irradiated cells were measured. After each anneal cycle all 12 cells were measured. Meter measurements of V_{oc} (open circuit voltage) and I_{sc} (short circuit current) were made at the same time. Figure 4 charts the results for V_{oc} for a typical irradiated cell showing the changes at each step in the experiment. V_{oc} shows a definite degradation after the electron irradiation, with only partial recovery after the first anneal cycle. This lead to the expansion of the anneal schedule from one minute at 500°C to five minutes at 500°C. In order to attempt further improvement, a third anneal was implemented at 600°C for five minutes. As is shown in figure 4, each anneal cycle resulted in an improvement in V_{oc} so that it recovered to within 95% of its original value. The proton irradiation caused another drop which was almost completely recovered in the subsequent anneal cycle. The V_{oc} measurements for the irradiated cells were corrected for the changes in the thermal controls. A typical example of the thermal control cells is shown in figure 5. There was little

change in V_{oc} for the thermal controls as they were subjected to the annealing cycles. The slight improvement has been noted in previous thermal cycle experiments to test high temperature tolerance and has been attributed to annealing of surface damage caused by application of the antireflection coating.

I_{sc} measurements for typical irradiated and thermal control cells are shown in figures 6 and 7 respectively. Figure 7 shows some degradation in I_{sc} as the cell was annealed. It is possible that this is due to the use of a new annealing fixture which may have deposited small quantities of contaminants on the cells during the anneal cycles. This would tend to affect the I_{sc} performance more than the V_{oc} since I_{sc} is more sensitive to light intensity. The irradiated cell in figure 6 shows almost complete recovery after the electron irradiation and partial recovery after the proton irradiation.

After the proton irradiation and again after the final annealing, dark IV curves were measured in an attempt to discover the thermal and radiation damage mechanisms. These measurements were made with a Keithley 236 source-measure instrument forcing currents from 0.1na to 10 ma and measuring voltage. Typical dark IV curves for one of the irradiated cells are shown in figure 8. The pretest curve is from one of the control cells. The curves labeled "post proton" and "post anneal 4" are from one of the irradiated cells. The control cell is used to show typical pretest characteristics because dark IV measurements were not made prior to the proton irradiation. These curves were modeled by two diodes, a series resistance, and a shunt resistance:

$$I = I_1(e^{q(V-IR_{series})/n_1kT} - 1) + I_2(e^{q(V-IR_{series})/n_2kT} - 1) + \frac{V}{R_{shunt}}$$

The slope of the dark IV curve for the control cell (pretest) corresponds to a value of n = 2 in the higher current portion (between 1μa and 1ma). This indicates a recombination region of the cell. The higher n value (2 - 3) in the lower currents from 1pa to 1μa indicates tunneling. The folding over of the curve above 1ma indicates a series resistance of about 25Ω for the control cell. The electron, proton radiation, and first three anneal cycles apparently had little effect on any of the dark IV parameters for this cell except series resistance, although this was not consistent from cell to cell. After the fourth anneal cycle, the folding over of the lower current portion of the curve indicates a decrease in the shunt resistance.

Similar dark IV curves are shown for one of the thermal control cells in figure 9. The trend for this cell is apparently an increase in the tunneling effect and a decrease in shunt resistance with additional time at high temperatures, although again this is not consistent from cell to cell. In some of the cells, the series resistance decreased with increasing time at high temperature. The parameters derived from the dark IV measurements are listed in table 1. Since dark IV curves were not measured in the earlier steps of the test program, the trends with increasing radiation and time at

temperature are not obvious. It is likely that these results are showing an intermixing of thermal and radiation effects.

Conclusions

The results of this experiment indicate that annealing of electron and proton induced radiation damage was taking place. It is apparent from the results that GaAs cell lifetimes in space applications can be extended by periodic thermal annealing of radiation damage. Complete recovery from radiation degradation may be possible with slight changes in cell design or careful design of annealing temperature profiles. Further study of the radiation and thermal damage mechanisms will be required to upgrade the cell design and determine optimum anneal profiles. These studies should include measurement of dark IV curves at varying temperatures before and after irradiation and thermal exposure in order to identify specific tunneling mechanisms. More thorough examination and modeling of the light IV curves may indicate additional damage mechanisms. Experiments with isochronal and isothermal annealing are then required in order to identify the most beneficial thermal profile. Again, measurement of dark IV curves at varying temperatures as well as light IV curves will help in detecting the intermediate stages of cell damage. Analysis of these will be important in determining the most effective thermal profile for annealing radiation damage.

References

[1.] A. C. Day, W. E. Horne and I. Arimura, IEEE Transactions on Nuclear Science NS-27, 1665 (1980).

[2.] M. B. Spitzer, J. Dingle, R. P. Gale, P. Zavracky, M. Boden and D. H. Doyle,*IEEE Photovoltaic Specialists Conference*, 930 (1988).

Cell	Type	Phase (post)	R_{shunt} (MΩ)	I_{01} (pa)	n_1	I_{02} (pa)	n_2	R_{series} (Ω)
17	thermal	anneal 3	505	62	2.39	14.2	2.15	238
18	thermal	anneal 3	9	5991	5.02	15.9	2.08	26
19	thermal	anneal 3		80	2.32	15.9	2.08	31
20	thermal	anneal 3	410	89	2.51	10.1	2.05	37
22	irradiated	p+	17	1308	3.30	75.6	2.25	126
23	irradiated	p+	124	174	2.48	18.1	2.02	
24	irradiated	p+		86	2.24	29.8	2.15	769
13	control	anneal 4		226	2.90	7.9	2.00	25
14	control	anneal 4	107	299	2.87	23.4	2.12	49
15	control	anneal 4	119	204	2.87	7.5	2.01	30
16	control	anneal 4	115	230	2.83	8.9	1.99	24
17	thermal	anneal 4		76	2.56	4.9	1.99	25
18	thermal	anneal 4	486	173000	8.45	37.6	2.20	29
19	thermal	anneal 4	72	469	3.04	14.4	2.07	26
20	thermal	anneal 4	286		2.62		2.01	25
22	irradiated	anneal 4						
23	irradiated	anneal 4	4	21560	8.26	0.5	1.74	30
24	irradiated	anneal 4	10	6075	5.68	1.4	1.84	27

Table 1. Dark IV Curve Parameters.

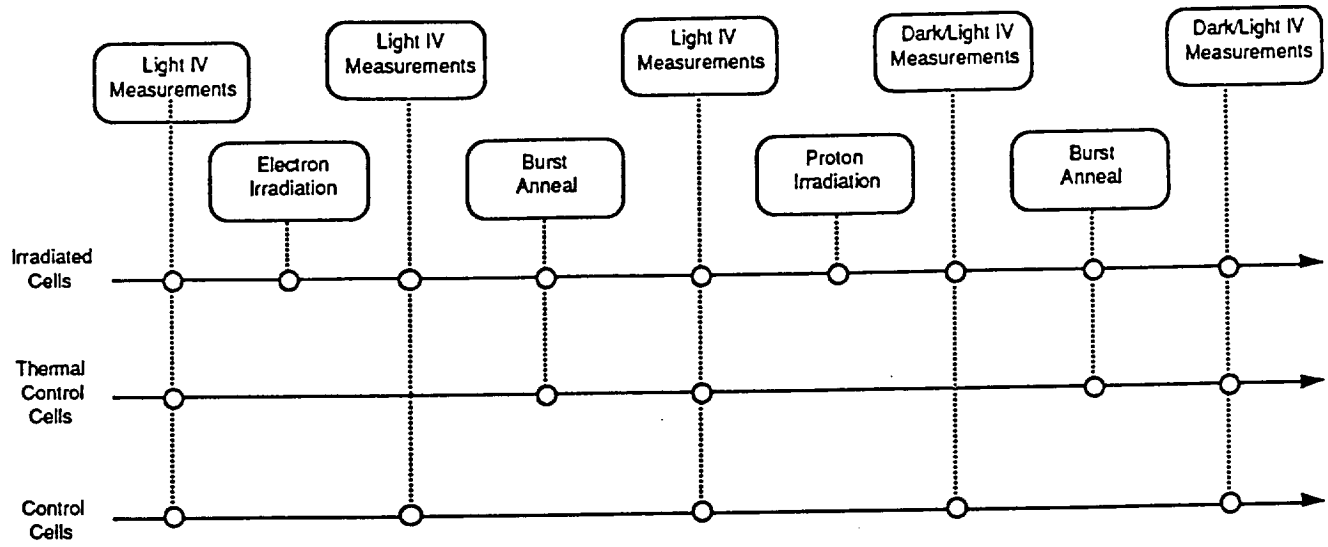

Figure 1. Burst Anneal Experiment Test Plan.

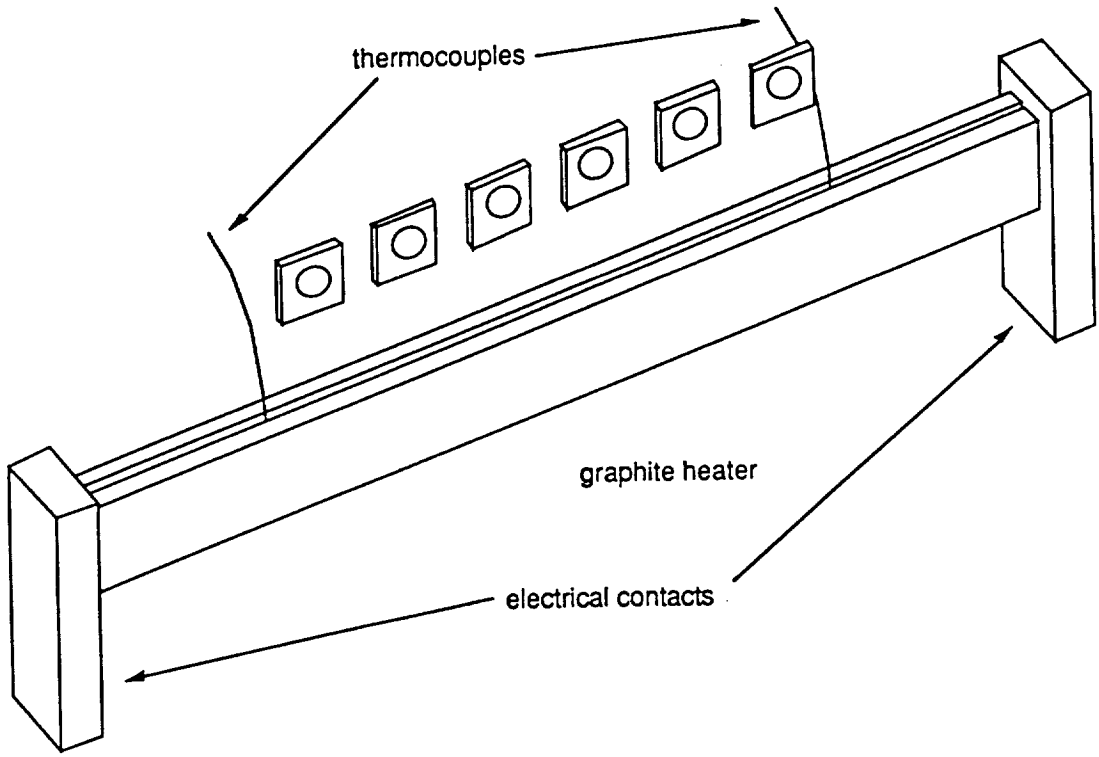

Figure 2. Annealing Test Fixture.

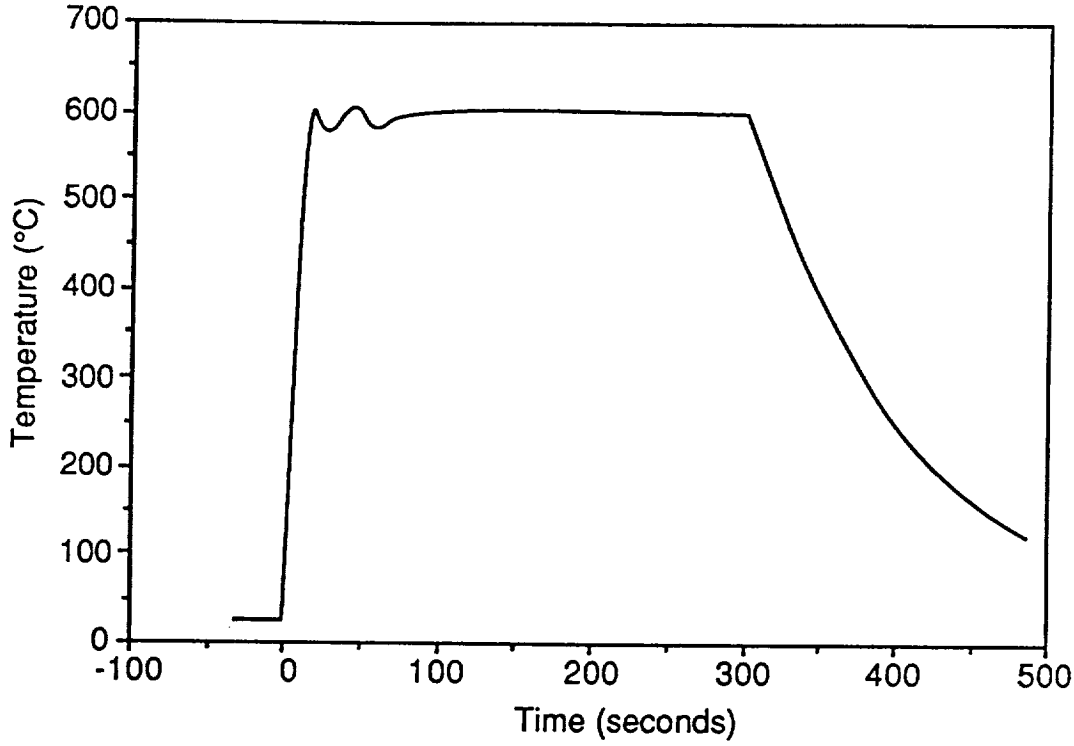

Figure 3. Typical Annealing Temperature Profile.

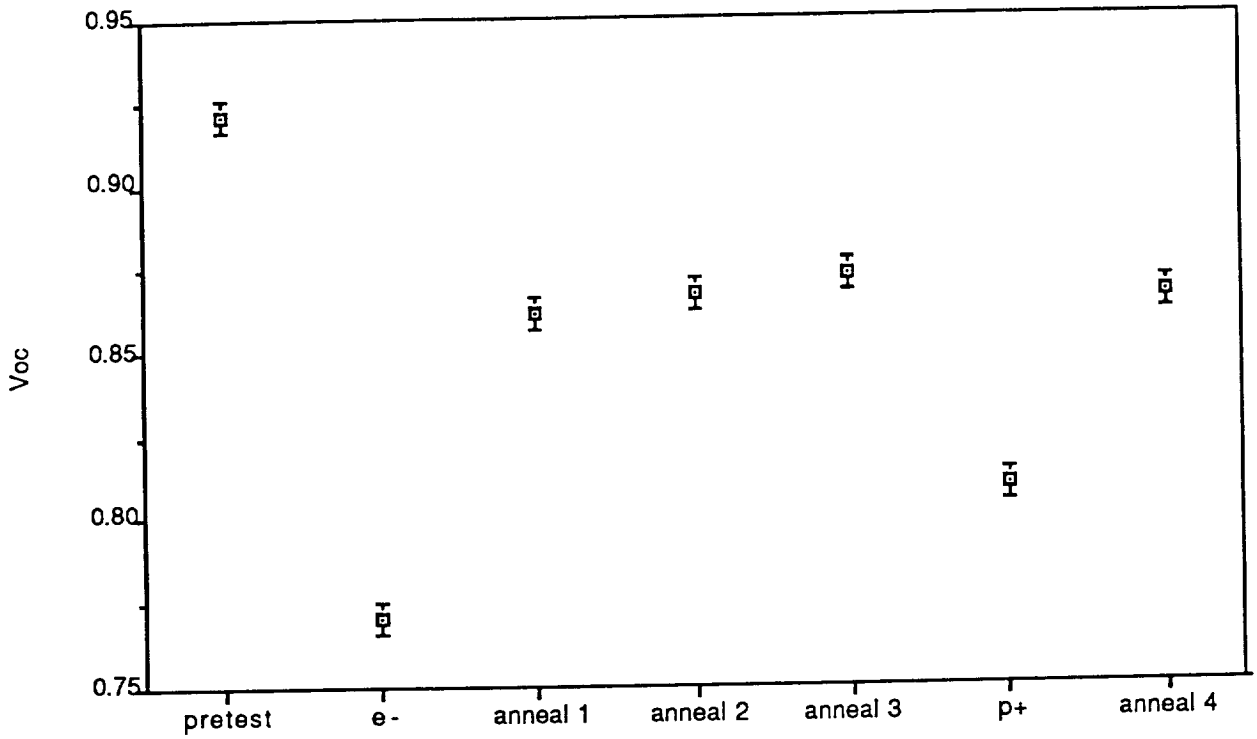

Figure 4. Irradiated Cell V_{OC} Changes.

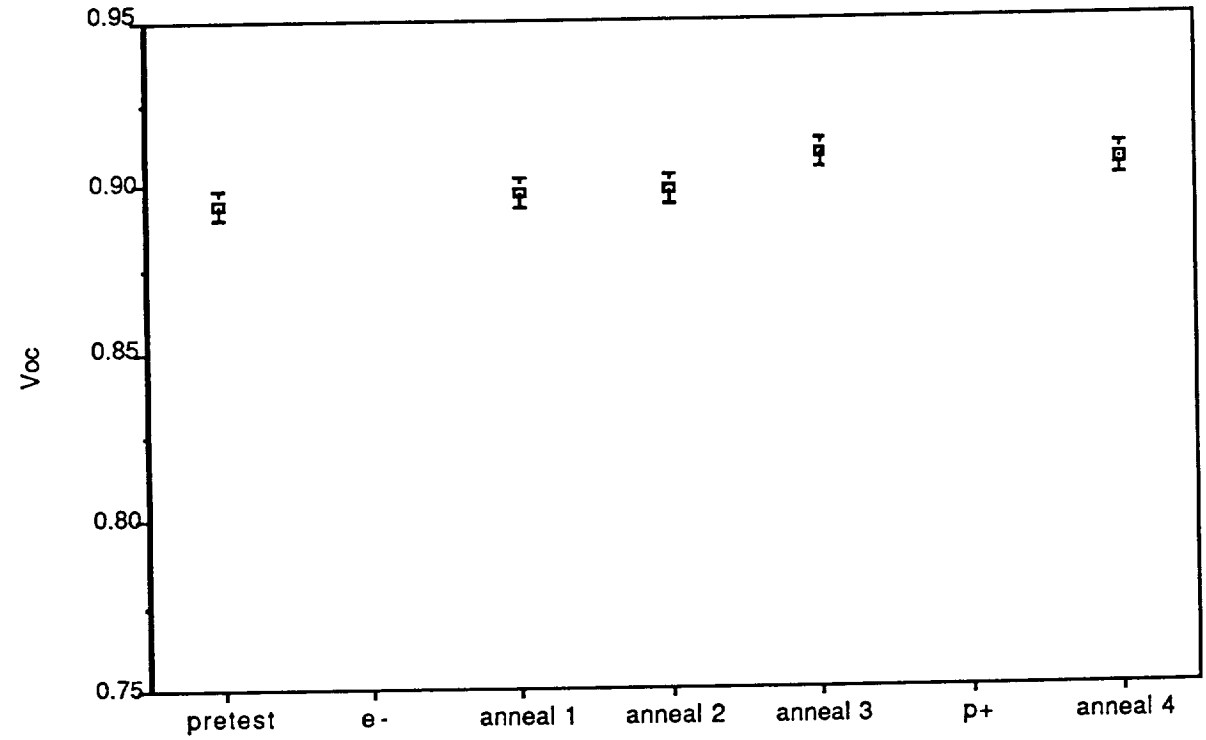

Figure 5. Thermal Control Cell V_{OC} Changes.

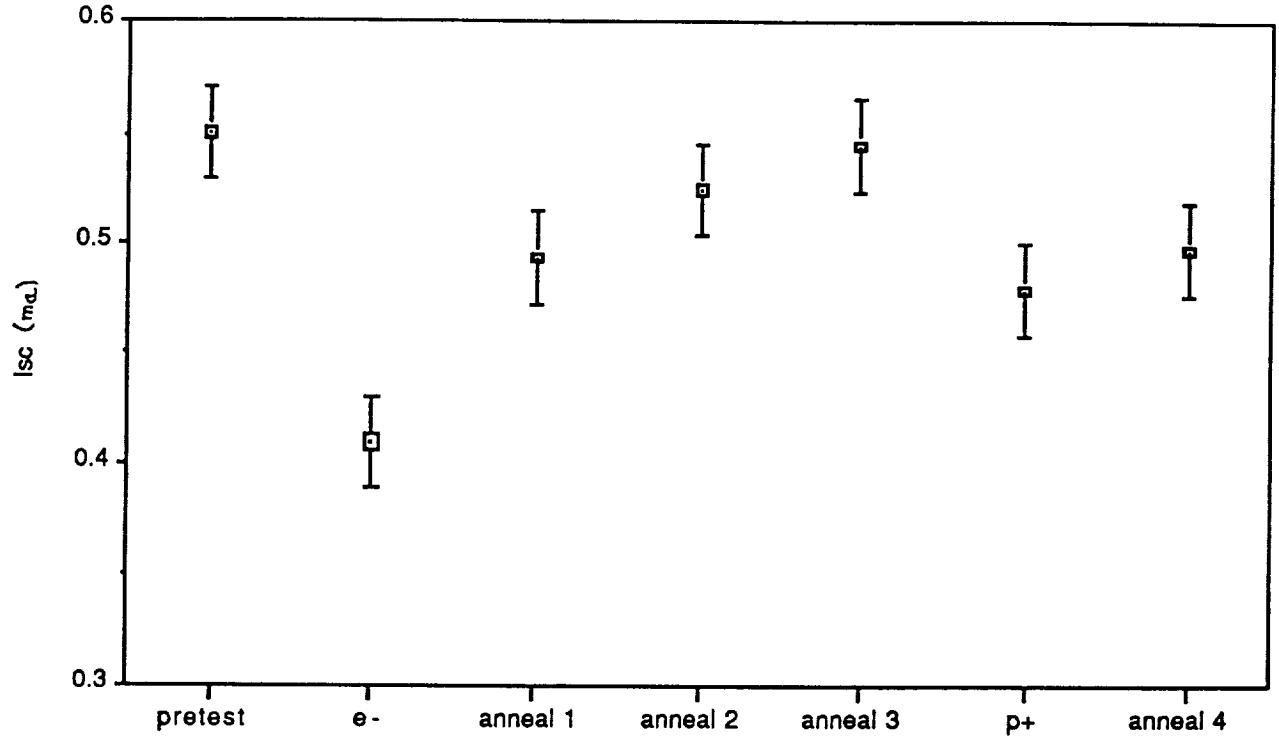

Figure 6. Irradiated Cell I_{SC} Changes.

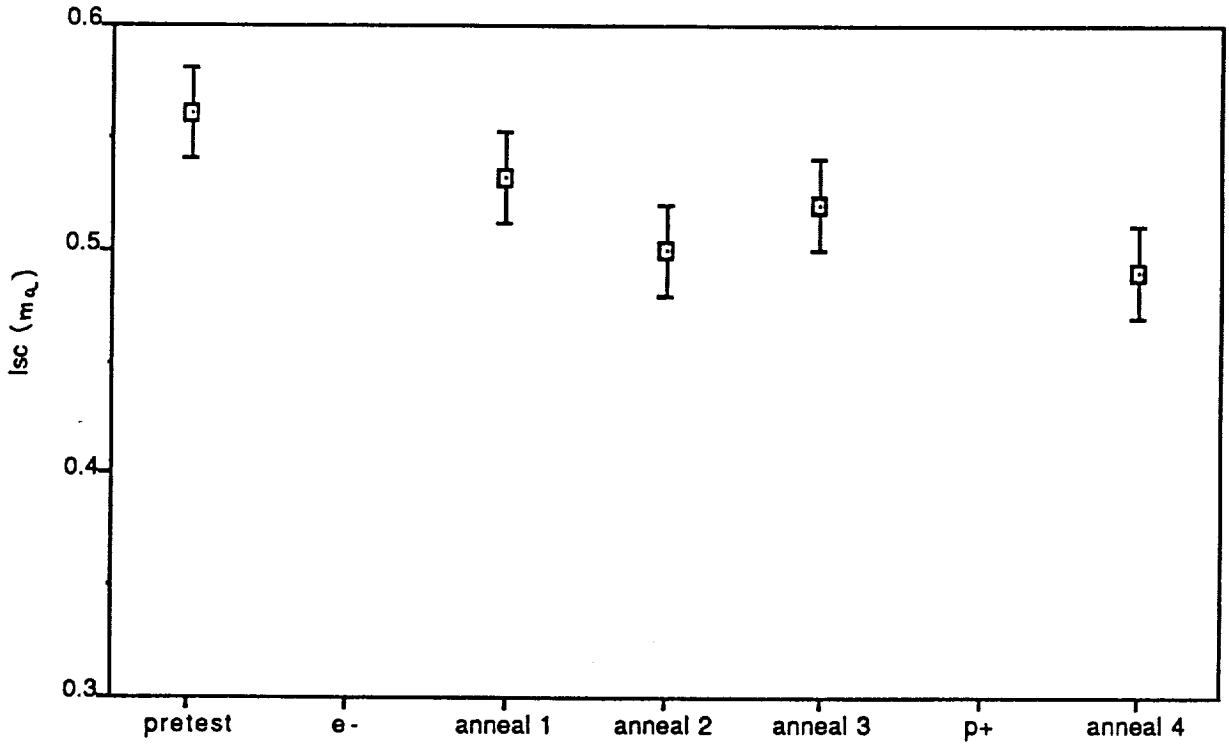

Figure 7. Thermal Control Cell I_{SC} Changes.

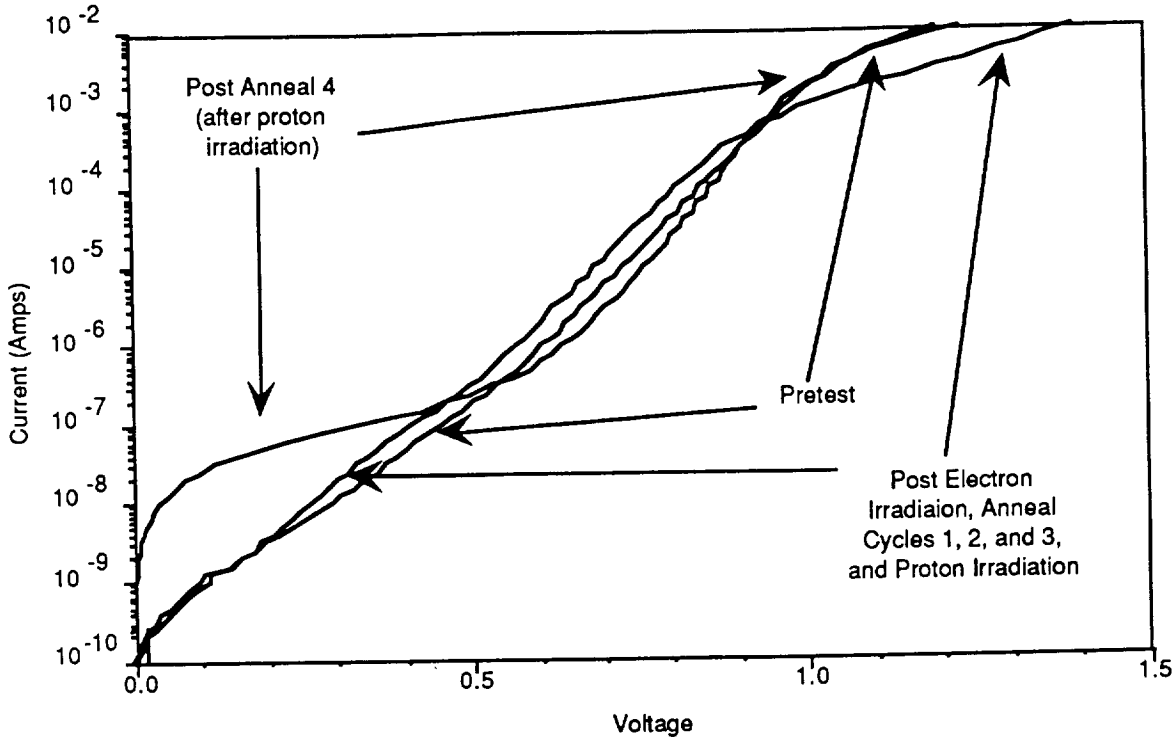

Figure 8. Irradiated Cell Dark IV Curve.

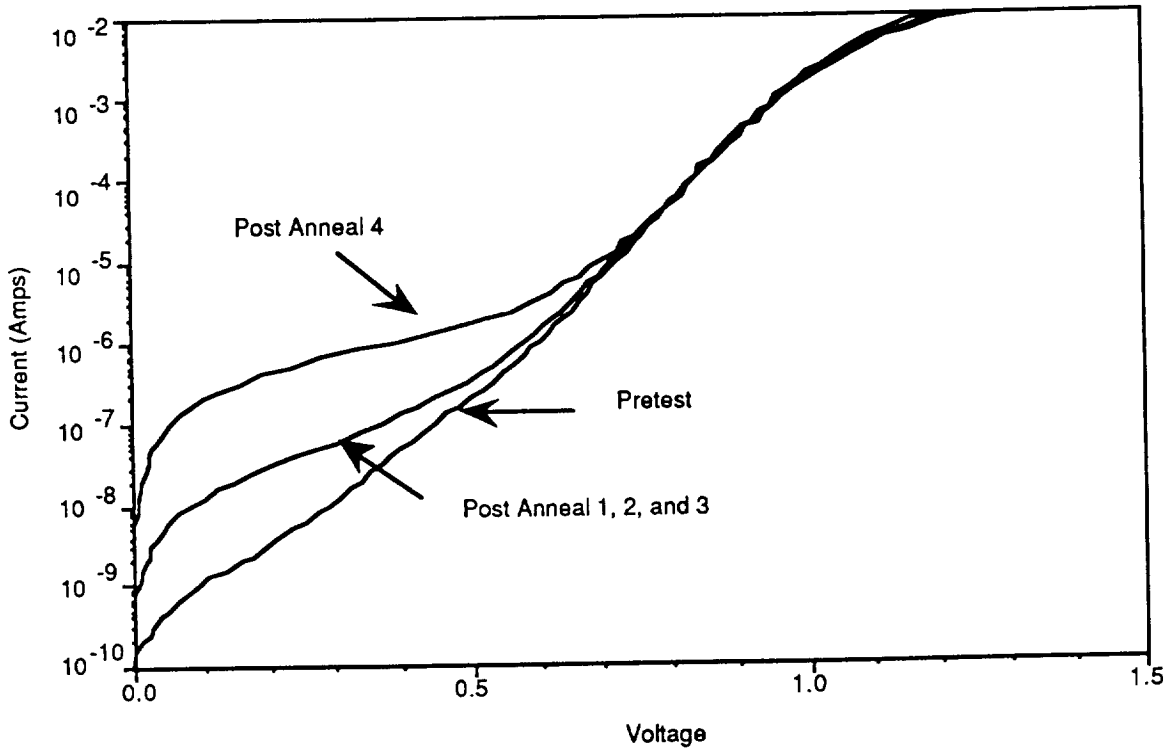

Figure 9. Thermal Control Cell Dark IV Curve.

Session 3
System Studies